

Thermodynamics of a spin- $\frac{1}{2}$ chain coupled to Einstein phonons

Alexander Bühler* and Götz S. Uhrig†

Institut für Theoretische Physik, Universität zu Köln, Zùlpicher Straße 77, 50937 Köln, Germany

Jaan Oitmaa‡

School of Physics, The University of New South Wales, Sydney, NSW 2052, Australia

(Received 28 July 2004; published 29 December 2004)

A high-order series expansion is employed to study the thermodynamical properties of a $S=1/2$ chain coupled to dispersionless phonons. The results are obtained without truncating the phonon subspace since the series expansion is performed formally in the overall exchange coupling J . The results are used to investigate various parameter regimes, e.g., the adiabatic and antiadiabatic limit as well as the intermediate regime, which is difficult to investigate by other methods. We find that dynamic phonon effects become manifest when more than one thermodynamic quantity is analyzed.

DOI: 10.1103/PhysRevB.70.214429

PACS number(s): 75.40.Cx, 05.10.-a, 75.10.Jm, 75.50.Ee

I. INTRODUCTION

In solid-state physics, all electronic degrees of freedom, such as charge or spin, are coupled to vibrations. Mostly, however, such a coupling does not influence the system's properties in a decisive way. This is different if the electronic degrees of freedom are essentially one dimensional. Then the phenomenon of a Peierls transition occurs: the system breaks translational invariance spontaneously by forming dimers.¹⁻⁶ The interest in a model of quantum phonons coupled to one-dimensional spin degrees of freedom in particular has been rekindled by the discovery of the inorganic spin-Peierls substance CuGeO_3 .⁷ Single crystals of high quality made investigations possible that were not possible for the long known organic spin-Peierls substances.²

Besides the spin-Peierls phenomenon a very strong coupling of spins and phonons can influence the quantitative physics of Mott insulators significantly if the superexchange coupling is small due to geometrical reasons. Examples are a 90° angle in the exchange path or a complicated superexchange process via large ligand groups. In these cases, a small change of the geometry implies a certain change of the coupling, which is very large *relative* to the unchanged coupling. Hence, the influence of phonons is much larger than usual. Examples for this mechanism, besides CuGeO_3 (Refs. 8 and 9), are $\text{SrCu}_2(\text{BO}_3)_2$ (Refs. 10 and 11) or $(\text{VO})_2\text{P}_2\text{O}_7$ (Refs. 12-14).

For the above reasons, it is of significant interest to provide reliable theoretical predictions for spin systems coupled to phonons. It is also clear that acoustic phonons will not have a significant influence because they alter the exchange paths relatively weakly. Thus we focus on optical phonons, which have a strong impact on the local geometry so that they can influence the exchange coupling significantly. For simplicity, we will consider dispersionless Einstein phonons. The aim of the present work is to compute the two fundamental thermodynamic quantities of spin systems, namely, the magnetic susceptibility and the specific heat, and to compare the results in the presence of a spin-phonon coupling to the results of static spin models. This comparison serves as a guideline to experimental analyses that attempt to identify the signatures of spin-phonon couplings.

The generic spin-phonon model introduced in Sec. II cannot be solved analytically. To the authors' knowledge, there are no analytical exact methods to treat extended systems of coupled spins and phonons if all energy scales shall be considered. Many numerical and approximate methods have been applied, such as density-matrix renormalization,¹⁵ continuous unitary transformations,¹⁶⁻¹⁸ exact diagonalization,¹⁹ linked cluster expansion,²⁰ renormalization group,²¹ and quantum Monte Carlo (QMC).^{18,22-26}

Two limits can be analyzed in more detail. In the adiabatic limit $\omega \ll J$ the spin system is assumed to be "fast" compared to the "slow" phonon system. Using approaches analogous to the ones applied by Pytte¹ and to the more detailed one by Cross and Fisher,³ the model in Eq. (1) can be mapped to a statically dimerized model.

The antiadiabatic limit $\omega \gg J$ can be handled by an appropriate mapping of the starting Hamiltonian to a frustrated spin model. Thereby, interactions of larger range are induced and the phonon frequency is renormalized.^{15-19,27} Above a critical frustration (e.g., a certain next-nearest-neighbor interaction), the system becomes gapped. This regime is reached for large values of the spin-phonon coupling. For small values of the spin-phonon coupling the system remains gapless. Note that we are dealing with a purely one-dimensional problem so that quantum fluctuations may prevent spontaneous symmetry breaking.

Concerning thermodynamic properties it could be shown that the magnetic susceptibility can be fitted by a frustrated spin model with temperature-independent couplings. But this approach fails for increasing values J/ω (Refs. 18 and 23).

Investigations of the regime between the adiabatic and the antiadiabatic limit with $\omega \approx J$ are difficult. So far, a renormalization group analysis²¹ and quantum Monte Carlo simulations^{18,23} have been done.

In the present paper, a spin-phonon model is studied using a linked-cluster expansion to derive thermodynamical properties, such as the specific heat C and the susceptibility χ . Zero temperature properties were determined previously.²⁰ The paper is organized as follows. Section II presents the model, some of its known properties, and the basic elements of the method employed. In Sec. III the results are analyzed. They are summarized in Sec. IV, where also open issues are identified.

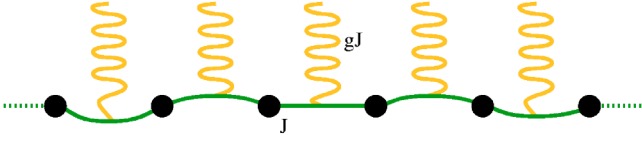


FIG. 1. (Color online) Schematic picture of the spin-phonon model as defined by Eq. (1).

II. MODEL AND METHOD

The isotropic spin- $\frac{1}{2}$ Heisenberg chain is extended by the coupling to local, dispersionless phononic degrees of freedom. The Hamilton operator reads

$$H = J \sum_i [1 + g(b_i^\dagger + b_i)] \mathbf{S}_i \mathbf{S}_{i+1} + \omega \sum_i b_i^\dagger b_i \quad (1a)$$

$$= H_{\text{SB}} + H_{\text{B}}. \quad (1b)$$

The magnetic exchange coupling is denoted by J , the coupling between the phononic subsystem and the magnetic subsystem is given by gJ , and the energy of the phonons is ω . The abbreviations H_{B} and H_{SB} are used in the following. The Hamiltonian in Eq. (1) represents the so-called bond-coupling model depicted schematically in Fig. 1. The phonons can be viewed to sit between the spin sites. They influence only one bond. Such a coupling can be motivated microscopically²⁸ for CuGeO_3 . But the main reason to choose the coupling as in Eq. (1) for our study is its simplicity.

In the antiadiabatic limit $J/\omega \rightarrow 0$, the critical spin-phonon coupling g_c for a phase transition from a gapless to a gapped phase is given by $g_c/\omega \approx 0.4682$ using the flow equation approach.¹⁸ Assuming a dimerized phase, the model was investigated at $T=0$ ²⁰ by a linked-cluster expansion which avoided any truncation of the phononic Hilbert space. But the starting point was the symmetry-broken dimerized phase at zero temperature. In the present paper, we emphasize the thermodynamical aspects of the model without broken symmetry. A series expansion about the limit of vanishing J/T is performed. The phononic subspace is treated exactly. No cutoff in the the phonon subspace is necessary. The resulting quantities are given as truncated series in J/T with full dependence on the remaining parameters, such as ω/T .

First we calculate the partition function Z of the spin-phonon system. Then, quantities, such as the free energy, the specific heat, or the susceptibility, can be derived easily. A traditional high-temperature series expansion is not possible because the expansion in the inverse temperature would lead to divergences in the phononic degrees of freedom. The limit of infinite temperature is not a well-defined starting point for bosons because the phonon occupation number diverges. For this reason, we choose to perform the formal expansion in the exchange coupling J . In this way, the phonon subspace is treated exactly for each given temperature. No truncation is necessary, and the full phonon dynamics is taken into account. To our knowledge, this is the first approach of a cluster expansion about the limit $J=0$ at finite temperatures, which avoids approximations in the phonon subspace.

We stress that the formal series in J coincides with the series for the magnetic subsystem in the inverse temperature if we set the spin-phonon coupling to zero: $g=0$. So it is not surprising that the obtained series bears many similarities to a high-temperature series. It is most reliable at high temperatures. The limit to vanishing temperature is difficult to describe.

The Hamilton operator from Eq. (1) is split into its diagonal part $H_0 = H_{\text{B}}$ and a perturbation V with

$$H = H_0 + JV = H_{\text{B}} + H_{\text{SB}} \quad (2a)$$

$$= \underbrace{\omega \sum_i b_i^\dagger b_i}_{H_0} + \underbrace{J \sum_i (1 + g(b_i^\dagger + b_i)) \mathbf{S}_i \mathbf{S}_{i+1}}_V. \quad (2b)$$

The diagonal part H_0 is trivially solvable; it describes free dispersionless (Einstein) phonons. The perturbation V includes the isolated magnetic part and the spin-phonon interaction. The standard way to treat such a problem is to change to the interaction representation where the off-diagonal perturbation governs the nontrivial part of the dynamics of the system. In this framework the partition function is given as an infinite series in the expansion parameter J by

$$Z = \text{tr}\{e^{-\beta H}\} \quad (3a)$$

$$= Z_0 \left(1 + \sum_{n=1}^{\infty} (-J)^n \int_0^\beta d\tau_1 \cdots \int_0^{\tau_{n-1}} d\tau_n \langle \tilde{V}(\tau_1) \cdots \tilde{V}(\tau_n) \rangle \right), \quad (3b)$$

where the following abbreviations are used. The unperturbed part H_0 in (2) leads to the contribution Z_0 of the partition function

$$Z_0 = \text{tr}\{e^{-\beta H_0}\} = 2^N \left\{ \prod_i \left(\sum_{n_i=0}^{\infty} e^{-\beta \omega n_i} \right) \right\} = 2^N z_0^N \quad (4)$$

with $z_0 = 1/(1 - e^{-\beta \omega})$ and the phonon occupation number $n_i = b_i^\dagger b_i$. The system size is denoted by N . The perturbation V given in the interaction representation as \tilde{V} reads

$$\tilde{V}(\tau) = e^{\tau H_0} V e^{-\tau H_0} \quad (5a)$$

$$= \sum_i \mathbf{S}_i \mathbf{S}_{i+1} [1 + g e^{\tau H_0} (b_i^\dagger + b_i) e^{-\tau H_0}] \quad (5b)$$

$$= \sum_i \mathbf{S}_i \mathbf{S}_{i+1} [1 + g (b_i^\dagger e^{\omega \tau} + b_i e^{-\omega \tau})]. \quad (5c)$$

The angular brackets in Eq. (3) are an abbreviated notation for

$$\langle \tilde{V}(\tau_1) \cdots \tilde{V}(\tau_n) \rangle = \frac{1}{Z_0} \text{tr}\{e^{-\beta H_0} \tilde{V}(\tau_1) \cdots \tilde{V}(\tau_n)\}. \quad (6)$$

As can be seen from the above equations the calculations for the partition function Z of the magnetic system and of the

phononic system factorize. In each order of expansion in J the contribution from the spin system can be evaluated separately from the phononic contributions.

Calculating the partition function in Eq. (3) requires repeated integrations over functions of the type

$$I(k, l; x_n) = x_n^k e^{lx_n} \text{ with } k \in \mathbb{N}_0, \quad l \in \mathbb{Z}, \quad x_n \in \mathbb{R}. \quad (7)$$

The resulting integrals can be solved exactly with

$$\int_0^{x_{n-1}} dx_n x_n^k e^{lx_n} = k! \left(-\frac{1}{l}\right)^{k+1} + \sum_{i=0}^k (-1)^i \times \frac{1}{l^{i+1}} \frac{k!}{(k-i)!} x_{n-1}^{k-i} e^{lx_{n-1}} \quad \text{for } l \neq 0, \quad (8a)$$

$$\int_0^{x_{n-1}} dx_n x_n^k = \frac{1}{k+1} x_{n-1}^{k+1} \quad \text{for } l = 0. \quad (8b)$$

These equations allow an iterative evaluation of the multiple integrals entering the partition function Z .

A useful check of the calculations is the limit $g=0$. This special case yields

$$Z_{g=0} = Z_{\text{isol. phonons}} Z_{\text{isol. spins}} = z_0^N Z_{\text{isol. spins}}. \quad (9)$$

Due to the one-dimensionality of the system under study a simple cluster algorithm will be used (for an instructive review see Ref. 29). Therein not only the connected clusters are calculated, but also the disconnected clusters. The unnecessary calculations of the disconnected cluster are not very costly, and we can save the bookkeeping overhead that would otherwise be required. The problem of subtracting subclusters occurring in the linked cluster expansion algorithm is replaced by the evaluation of the lattice constants for a given cluster.

III. RESULTS

Here the results for the specific heat C and for the susceptibility χ are presented in Secs. III A and III B. Section III C is dedicated to the comparison of the results from static spin models and those from the spin-phonon model.

The bare truncated series provides a first impression of the behavior of the considered quantities for various sets of parameters. But for quantitative predictions the truncated series are not sufficient, as will be seen in the following. Extrapolation techniques are necessary to improve the representation of the results for larger values of J . It turns out that the description of higher temperatures is easily possible whereas the extrapolation becomes ambiguous at low temperatures. We attribute this behavior to the fact that the phononic and magnetic subsystems behave at higher temperatures more and more independently. Then our series is essentially a high-temperature expansion for the magnetic system, which is known to work well for higher temperatures. For low temperatures, however, possible long-range effects set in, which elude our approach.

We benchmark our results relative to QMC data for selected sets of parameters.²⁵

The results for the spin-phonon model are compared to those of pure spin systems. As a reference, the exact result of the isotropic Heisenberg model³⁰⁻³² is depicted in the figures for the susceptibility. The specific heat is compared to the specific heat of free phonons plus the exactly known result for $C(T)$ for the Heisenberg model.³²

The coefficients of the series expansion results are available upon request.

A. Specific heat

A detailed study of the magnetic properties of the system under consideration also includes the investigation of the specific heat. Besides the magnetic susceptibility the specific heat is an observable that can be experimentally easily measured and theoretically easily calculated. A direct comparison between theory and experiment is often hindered by the fact that the phononic degrees of freedom dominate the specific heat. Our model (1) takes the influence of a strongly coupled acoustic phonon into account. The additional contribution of acoustic phonons is beyond the scope of the present investigation. We assume that the contribution of the acoustic phonons is indeed additive so that it can be accounted for if the lattice vibrations are known, e.g., from a dynamic lattice model.

The specific heat $C(T)$ is obtained from the results for the free energy per site f obtained from the partition function Z using standard relations from statistical physics

$$f = F/N = -\frac{1}{\beta N} \ln Z. \quad (10)$$

The free energy could be computed to order 13 in J . To this end, the contribution of 214 connected and 470 disconnected clusters had to be evaluated. To illustrate the result the first orders of the free-energy series are given

$$\begin{aligned} -\beta f &= \frac{1}{N} \ln(Z) \\ &= \ln z_0 + J^2 \left(\frac{3}{32} \beta^2 + \frac{3}{16} \frac{g^2 \beta}{\omega} \right) \\ &\quad + J^3 \left(\frac{1}{64} \beta^3 + \frac{3}{32} \frac{g^2 \beta^2}{\omega} \right) + J^4 \frac{1}{256} \left\{ -\frac{5}{4} \beta^4 + 6 \frac{g^2 \beta^3}{\omega} \right. \\ &\quad \left. + \left[(24z_0^2 - 24z_0 + 6) \frac{g^4}{\omega^2} + (-48z_0 + 24) \frac{g^2}{\omega^2} \right] \beta^2 \right. \\ &\quad \left. + \left[(12 - 24z_0) \frac{g^4}{\omega^3} + 48 \frac{g^2}{\omega^3} \right] \beta \right\} + \mathcal{O}(J^5). \quad (11) \end{aligned}$$

To obtain a detailed insight in the behavior of the specific

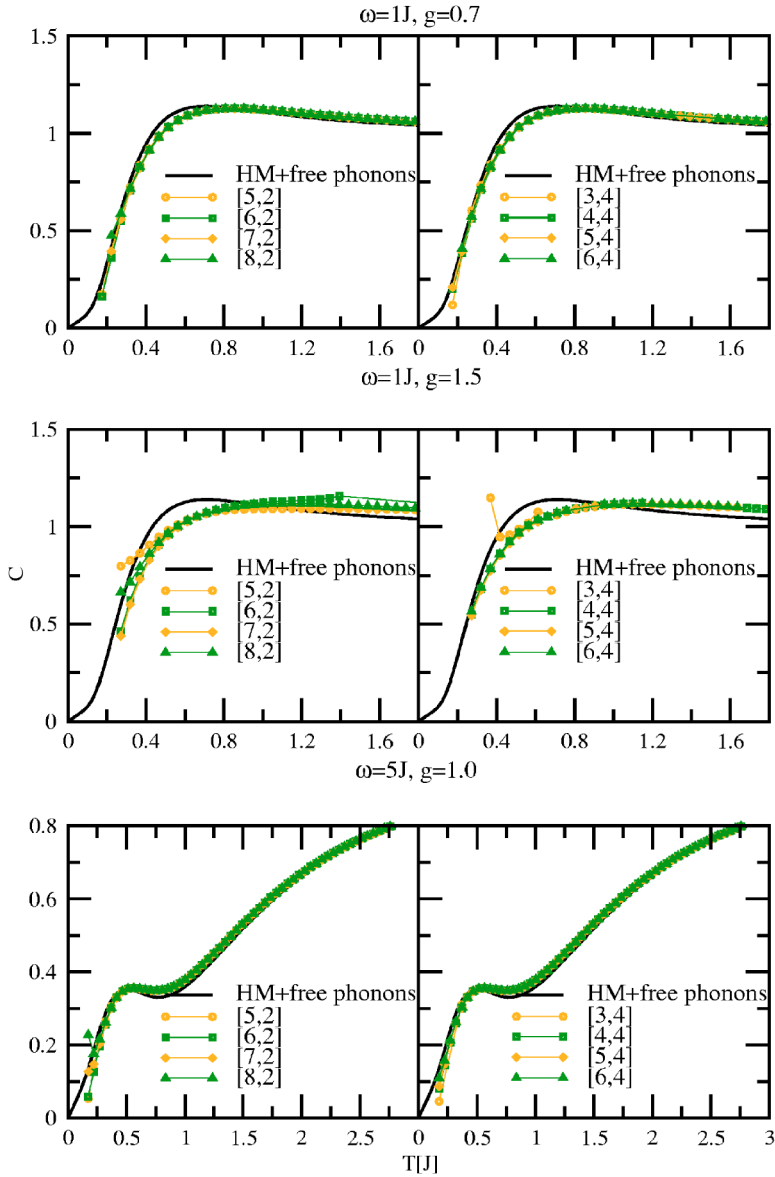


FIG. 2. (Color online) Dlog-Padé extrapolations of the specific heat. Various extrapolations are compared for three different sets of parameters.

heat, Dlog-Padé extrapolations are used. The truncated series alone are not appropriate for temperatures below $T < J$ (not shown). Figure 2 depicts the extrapolation results of the specific heat compared to a superposition of the free phonon part of the specific heat given by

$$C_B = (\beta\omega)^2 \frac{e^{-\beta\omega}}{(1 - e^{-\beta\omega})^2} \quad (12)$$

and the exactly known result C_S for the isotropic Heisenberg model. Various parameter sets are shown. Simple Dlog-Padé extrapolations in J are used for each temperature point. To this end, the exactly known result of the free phonons is subtracted from the series obtained. The resulting expression is extrapolated; it starts in second order in J . Starting from results for the partition function in order 13 in J , the maximum order of extrapolation of the remaining specific heat is 10. Ordinary Padé extrapolations would allow a maximum order of 11, but due to the differentiation for the Dlog-Padé extrapolations, one additional order is lost. After the extrapo-

lation, the free-phonon contribution is added again. This procedure is chosen to deal with series that behave qualitatively, such as the high-temperature series for pure spin systems.

In Fig. 2 the results for three different sets of parameters $\omega=1J$, $g=0.7$ (upper panels), $\omega=1J$, $g=1.5$ (middle panels), and $\omega=5J$, $g=1$ (lower panels) are shown. The left plots depict the $[n,2]$ and the right plots the $[n,4]$ extrapolations. In the $[n,m]$ scheme the logarithmic derivative is approximated by a rational function, where the polynomial in the numerator has the degree n while the one in the denominator has the degree m .

The $[n,2]$ and the $[n,4]$ schemes converge very well. The $[n,4]$ extrapolations are more stable in the low-temperature regime for both parameter sets. Hence, this scheme is used in the following. The range of validity can be specified by $T \geq 0.15J$ as long as the spin-phonon coupling is smaller or of the same order as ω . For values of $gJ/\omega > 1$ the extrapolations suffer often from spurious poles. In the middle panels the defective extrapolations are visible. The schemes $[5,2]$, $[6,2]$, and $[3,4]$ yield extrapolations that differ significantly

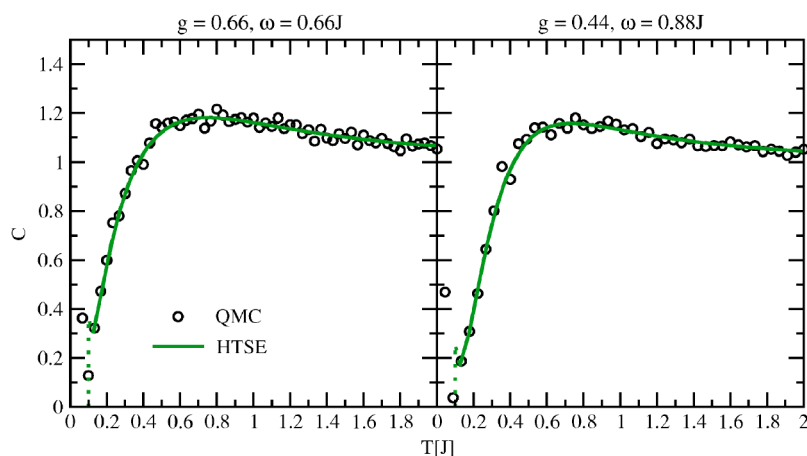


FIG. 3. (Color online) Dlog-Padé extrapolations of the specific heat compared to QMC data. The left plot shows data for the values $g=0.66$, $\omega=0.66J$, and the right plot depicts the parameters $g=0.44$, $\omega=0.88J$.

from the other schemes considered. This is due to spurious poles in the integration interval with respect to J . For [6, 2] even temperatures above $T \approx J$ are not described reliably.

For small spin-phonon coupling g the specific heat is well described by the sum of the phononic C_B and the magnetic specific heats C_S of the isolated subsystems (cf. first row of panels in Fig. 2). Increasing the spin-phonon coupling shifts the specific heat to larger values (cf. second row of panels in Fig. 2). In this temperature regime ($T > J$) already the truncated series yield trustworthy results.

Fixing the spin-phonon coupling g and increasing the phonon frequency ω weakens the visible effect of the phonon dynamics (cf. third row of panels in Fig. 2). This is to be expected because the phononic subsystems become more rigid, so that it will not be influenced significantly by the spin systems and vice versa.

Finally, we compare the extrapolated results from the cluster expansion in J to data obtained by QMC. Figure 3 depicts two sets of parameters of the [6, 4] scheme and the corresponding QMC data. The left panel shows the result for $g=0.66$ and $\omega=0.66J$. This parameter set implies that the system is gapped.¹⁸

In the right-panel results are depicted for $g=0.44$ and $\omega=0.88J$, which implies a gapless phase. The statistical error of the QMC data can be estimated from the spread of the data points. The extrapolated series yield smooth, continuous results that agree very well with the QMC data. For temperatures below $T/J \approx 0.15$ the dotted lines refer to defective extrapolations, which are depicted for illustration. These extrapolations are known to yield unreliable results beforehand because the extrapolants display spurious poles in the integration interval of J . Note that each temperature requires an extrapolation. The extrapolations at higher temperatures turn out to be very stable and not defective so that reliable results can be obtained for temperatures $T \gtrsim 0.15J$. For lower temperatures, the extrapolations are contaminated by spurious poles and should not be trusted.

B. Susceptibility

The magnetic susceptibility χ is of special interest because it is most easily accessible experimentally. Very often static models, such as the dimerized and/or frustrated spin

chain, can already yield a good description of the susceptibility of one-dimensional systems. Two cases are conceivable: either the appropriate model is indeed a static spin model or the static spin model should be seen as an effective model that incorporates the effects of the spin-phonon coupling. Of course, it only makes sense to distinguish both cases if there are other experimental probes to discriminate between them. This will be elucidated in Sec. III C.

In the antiadiabatic limit $\omega > J$, detailed investigations of the susceptibility were done. The spin-phonon chain could be mapped to a frustrated spin chain with temperature-dependent exchange couplings.¹⁸ The corresponding susceptibility could be obtained from a high-temperature series expansion.³³ It was shown that χ is only little affected by the temperature dependence of the coupling constants. Thus it can be neglected and a static model is indeed well justified. This finding agrees with previous results.¹⁴ It explains, for instance, why the magnetic susceptibility of CuGeO_3 can be fitted so surprisingly well by a static frustrated Heisenberg model.^{34–36}

We expect that the mapping to a static spin model works less well in the crossover regime to the adiabatic limit $\omega \lesssim J$. There the effects of the phonon dynamics should be more clearly visible. We will return to this question in Sec. III C.

The series expansion of the susceptibility is obtained from the previous considerations by incorporating an external magnetic field. In a first step, the coupling of this field to the spins is added to the unperturbed Hamilton operator H_0 that leads to a modified free-energy series expansion. In a second step, the susceptibility can be derived from the free-energy series.

The unperturbed part H_0 of the Hamilton operator (2) is extended by a magnetic field term leading to

$$H_0 = \omega \sum_i b_i^\dagger b_i - h \sum_i S_i^z = H_B - hM \quad (13)$$

with the magnetic field h given in units of $g\mu_B$. The additional term proportional to the magnetization M commutes with the free phonon part H_B and with the perturbation V as given in Eq. (2). Thus, the expression for $\tilde{V}(\tau)$ in Eq. (5) is

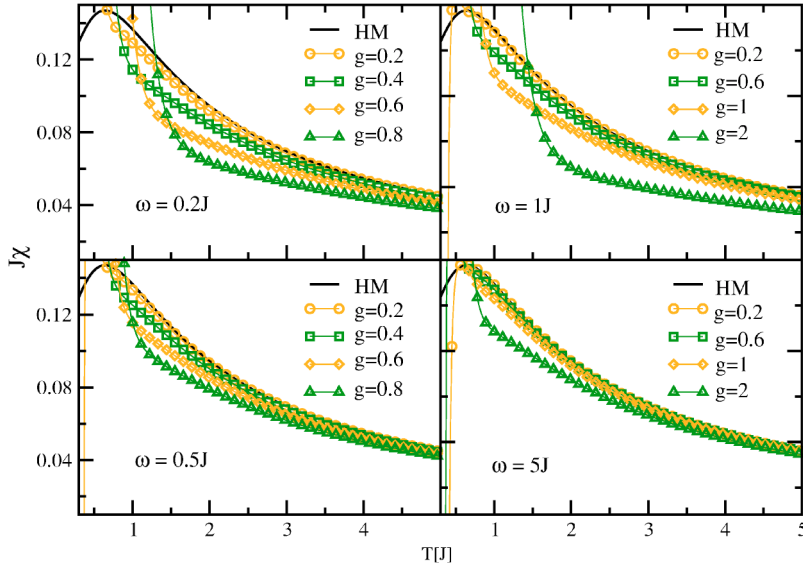


FIG. 4. (Color online) Truncated series of the susceptibility. Various sets of parameters are shown. The exactly known result for the Heisenberg model serves as a reference. The left panels illustrate the adiabatic limit whereas the right panels show the results in the antiadiabatic limit.

unchanged compared to the calculation of the specific heat. The magnetic field is included in H_0 .

The formal expression Eq. (3) for the partition function is unchanged. From Eq. (13) we deduce the zeroth-order contribution Z_0 , which now reads

$$Z_0 = \text{tr}(e^{-\beta H_0}) = \text{tr}(e^{-\beta H_B} e^{\beta h M}) \quad (14a)$$

$$= z_0^N \left[2 \cosh\left(\frac{\beta h}{2}\right) \right]^N. \quad (14b)$$

Taking the logarithm of the partition function Z yields

$$\frac{1}{N} \ln Z = \ln z_0 + \ln \left[2 \cosh\left(\frac{\beta h}{2}\right) \right] \quad (15a)$$

$$+ \sum_{n=1}^{\infty} (-J)^n \left\{ \int_0^{\beta} d\tau_1 \cdots \int_0^{\tau_{n-1}} d\tau_n \langle \tilde{V}(\tau_1) \cdots \tilde{V}(\tau_n) \rangle \right\} \quad (15b)$$

with z_0 as given in Eq. (4). The angular brackets $\langle \cdots \rangle$ denote the coefficients proportional to N in the trace [see Eq. (6)]. To derive the susceptibility, the above equation has to be differentiated twice with respect to the magnetic field h . Finally h is set to zero

$$T\chi = \frac{1}{\beta^2} \left. \frac{\partial^2}{\partial h^2} \left(\frac{1}{N} \ln Z \right) \right|_{h=0}. \quad (16)$$

The susceptibility could be computed up to order 12 in J . The contribution of 2242 connected and 2810 disconnected clusters had to be evaluated. To illustrate the result the first orders of the susceptibility series are given

$$\begin{aligned} T\chi = & \frac{1}{4} - \frac{1}{8}J\beta - \frac{1}{16}J^2\beta\frac{g^2}{\omega} + \frac{1}{96}J^3\beta^3 \\ & + J^4\frac{1}{1536} \left\{ 5\beta^4 + 24\frac{g^2\beta^3}{\omega} \right. \\ & + \left[(-72z_0^2 + 72z_0)\frac{g^4}{\omega^2} + (-96 + 192z_0)\frac{g^2}{\omega^2} \right] \beta^2 \\ & \left. + \left[(72z_0 - 36)\frac{g^4}{\omega^3} - 192\frac{g^2}{\omega^3} \right] \beta \right\} + \mathcal{O}(J^5). \quad (17) \end{aligned}$$

In Fig. 4, the truncated susceptibility series are depicted for various parameter sets. The energy scales are given in units of the magnetic exchange coupling J . The exact result of the Heisenberg model serves as a reference to illustrate the effects of the additional coupling to the phonons. The general feature that the results diverge for temperatures below $T \lesssim 1.5J$ is expected for the truncated series. But the qualitative behavior of the susceptibility is already discernible.

The left panels depict the adiabatic regime and the right panels illustrate the antiadiabatic limit. The following conclusions can be drawn from the truncated series in the temperature regime $T \gtrsim 1.5J$. Fixing the phonon frequency ω the overall height of the susceptibility is lowered for increasing spin-phonon coupling g . Such a behavior can be understood in a mean-field treatment of the spin-phonon coupling. For increasing g the effective coupling $J_{\text{eff}} = J(1 + g\langle b^\dagger + b \rangle)$ increases. This shifts the whole susceptibility to lower temperatures compared to the result of the Heisenberg model with the bare magnetic exchange J , cf. discussion in Ref. 18.

For fixed spin-phonon coupling and increasing phonon frequency ω this effect becomes less pronounced. For increasing phonon frequency the magnetic and phononic degrees of freedom decouple more and more because the phonon system becomes increasingly rigid so that it is influenced less and less by the magnetic subsystem. Concomitantly, the spin system is less influenced by the phononic subsystem. Thus, for fixed g and $\omega \rightarrow \infty$ the magnetic properties are dominated by the antiferromagnetic Heisenberg model.

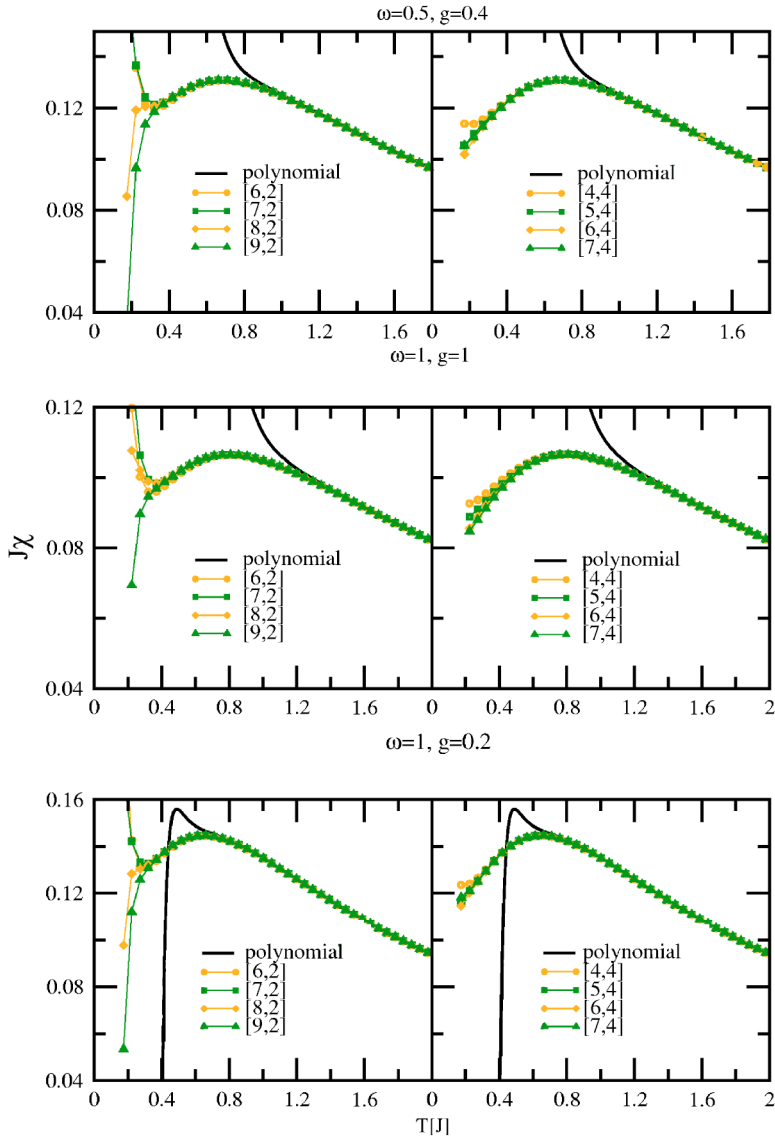


FIG. 5. (Color online) Dlog-Padé extrapolations of the susceptibility. Various extrapolation schemes are compared for three different sets of parameters. The parameters in the first two rows of panels correspond to the gapped regime whereas the lowest row depicts results in the gapless regime.

The truncated series fails to reproduce the very significant maximum of $\chi(T)$ (cf. Fig. 4). This maximum serves as a landmark for many experimental analyses. Thus the height and the position of the maximum are of great interest. Extrapolations are necessary to extend the representation of the results beyond the radius of convergence of the truncated series so that the maximum can be captured reliably. For the susceptibility the same extrapolation techniques are applied as for the pure spin models described in Ref. 33. Basically, the truncated series is extrapolated using Dlog-Padé approximants in an Euler-transformed variable. In contrast to the pure spin models, the extrapolations of the results of the spin-phonon model are not performed in the inverse temperature β , but in the magnetic exchange coupling J . For each temperature a separate extrapolation in J has to be done. Using standard routines from computer algebra programs, this does not pose any more problems than the previous extrapolations in β .

A more serious restriction concerns the behavior at large values of J . For the pure spin systems it was very efficient to bias the extrapolations in the inverse temperature such that the known low-temperature behavior was captured (see, e.g., Ref. 33). For the spin-phonon system, however, much less is known about the excitations at low energies. From the phase diagram depicted in Ref. 18, it can be deduced whether the system is gapped or gapless. But the precise value of the gap, let alone the form of the dispersion, are not available in the limit $J \rightarrow \infty$. Note that for the present expansion it is this limit that we need to understand, not the limit $T \rightarrow 0$ as in the high-temperature series. Hence, we do not attempt to bias our expansions in their behavior at large values of J . But an improved understanding of the limit $J \rightarrow \infty$ will certainly help to obtain even better extrapolations.

Figure 5 shows an overview over the susceptibilities obtained from unbiased Dlog-Padé extrapolations for three different sets of parameters. The upper two rows correspond to

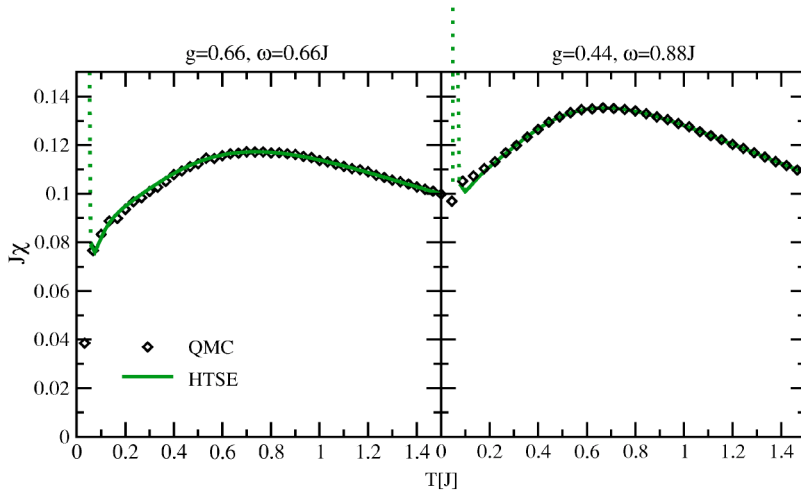


FIG. 6. (Color online) Dlog-Padé extrapolations of the susceptibility compared to QMC data. The left plot shows data for the values $g=0.66$ and $\omega=0.66J$ (gapped phase), and the right plot depicts data for the values $g=0.44$ and $\omega=0.88J$ (gapless phase).

results in the gapped regime whereas the parameters in the last row correspond to the gapless regime (see the phase diagram in Ref. 4). The left panels depict the extrapolations of the form $[n, 2]$ and the right panels the extrapolations of the form $[n, 4]$.

The position and the height of the maximum are described reliably by both extrapolation schemes $[n, 2]$ and $[n, 4]$. This conclusion is based on the agreement of the results for different orders n in Fig. 5. We observe that the $[n, 4]$ extrapolations converge better than the $[n, 2]$ extrapolations for increasing order. Higher values of m in the general $[n, m]$ scheme or odd values of m are likely to imply spurious poles. Thus, the $[n, 4]$ scheme is used in the following to represent the susceptibility for all parameter sets shown in this paper.

For temperatures $T < 0.2J$ no results are depicted due to spurious poles in the extrapolations in J . The range of validity of the $[n, 4]$ extrapolations can be estimated to be at least $T \geq 0.25J$ independent of the parameter sets that we analyzed in our investigations.

Finally, we illustrate the reliability of our extrapolations by a comparison to QMC data. For two different sets of parameters, Fig. 6 displays the $[7, 4]$ extrapolations of the series and the corresponding QMC data. The values $g=0.66$ and $\omega=0.66J$ in the left panel imply that the system is gapped. The values $g=0.44$ and $\omega=0.88J$ in the right panel correspond to the gapless regime. The agreement between the extrapolated series results and the QMC data is very good. For temperatures above $T/J \geq 0.2$ the results coincide. Below $T \leq 0.2J$ the QMC data and the series data deviate from each other. At present, we cannot decide whether the deviations for $0.1J < T < 0.2J$ are due to problems in the QMC simulation, such as statistical errors or finite-size effects, or whether they are due to problems in the series extrapolations. Below $T \approx 0.1J$, spurious poles occur in the extrapolated integrands leading to defective extrapolations. For illustration, these defective extrapolations are shown as dotted lines in Fig. 6.

We emphasize that the convincing agreement of the QMC, and the series results in the regime $T \geq 0.2J$ supports the reliability of these results. In particular, the position and the height of the important maximum of the susceptibility are described quantitatively.

C. Comparison to static spin models

Here, the importance of the spin-phonon dynamics shall be highlighted. As mentioned before it is often possible to describe the properties of a spin-phonon model by a static spin model alone, in particular in the antiadiabatic regime. It is to be expected that the effects of the dynamic nature of the spin-phonon coupling are most prominent in the regime where all energies are of similar magnitude. To provide evidence for this hypothesis we perform the following “theoretical” experiment.

We start from the extrapolated series data for $g=1$ and $\omega_0=J$ (see symbols in Fig. 7). These data shall serve as “experimental” input, which we will then analyze using static spin models. The static spin model considered here is the frustrated and dimerized spin chain given by

$$H = J \sum_i \{ [1 + \delta(-1)^i] \mathbf{S}_i \mathbf{S}_{i+1} + \alpha \mathbf{S}_i \mathbf{S}_{i+2} \}. \quad (18)$$

In this way, we imitate the standard procedure one would apply to experimental data. The objective is to see to which

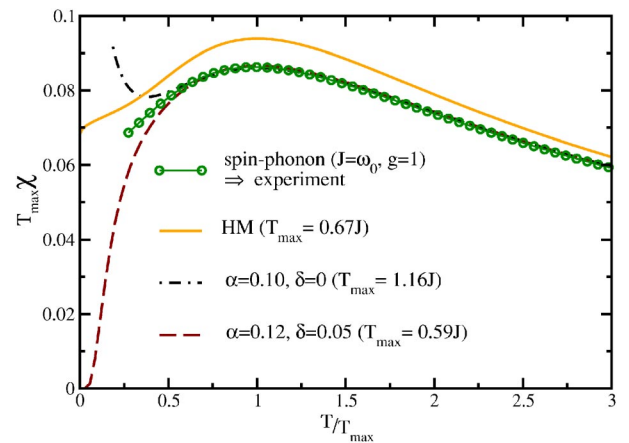


FIG. 7. (Color online) “Theoretical” experiment: The data for $g=1$ and $\omega_0=J$ (symbols) are taken as (mock) experimental input. It is fitted by the susceptibility of static spin model (solid lines). The temperature T_{\max} denotes at which temperature the susceptibility has its maximum; this value sets the natural energy scale of the problem.

extent such an analysis yields agreement. In particular, we are interested to see where such a description remains unsatisfactory. Such an unsatisfactory description based on static spin models is the signature of the dynamic nature of the spin-phonon coupling.

In Fig. 7 the experimental susceptibility is analyzed by the susceptibility of static spin models [i.e., the isotropic Heisenberg model (HM)], the purely frustrated spin chain, and the dimerized and frustrated chain. Obviously, the HM is not appropriate to describe the data depicted by the symbols. But the other two parameter sets ($\alpha=0.1, \delta=0$) and ($\alpha=0.12, \delta=0.05$) describe the experiment data very well for not too low temperatures (i.e., $T > 0.5T_{\max}$). This temperature regime corresponds to the range of temperatures where the extrapolated high-temperature series for the dimerized and frustrated spin chain are reliable.³³

Of course, it is possible to distinguish between different models if reliable (experimental) data down to low temperatures are available. In practice, however, this is often not the case because the data at low temperatures can be contaminated by impurity effects or other imperfections, such as inclusions of other phases, or simply the presence of other structural elements in the sample. In such a situation, the determination of the appropriate microscopic model is difficult and ambiguities are hard to avoid.

One way to make progress is to use the parameter set determined from the susceptibility data and to examine whether other properties can be understood with the same parameter set as well. Here we choose to study the specific heat. In the upper panel of Fig. 8 the phonon frequencies are assumed to be known *a priori*; therefore, the free phonon contribution added is the one for this known frequency $\omega = \omega_0$. Clearly, none of the static spin models describes the susceptibility data *and* the specific data satisfactorily. From the knowledge of both quantities, compelling evidence can be deduced that a dynamic spin-phonon coupling must be present.

But the situation can be less advantageous in practice. Let us assume that we do not possess knowledge about the frequency of the phonon to which the spin system may or may not be coupled. Then this frequency could be seen as an additional fit parameter. This view point was adopted in the lower plot in Fig. 8. The parameter set ($\alpha=0.1; \delta=0$) of the dashed-dotted curve can be clearly discarded. The parameter set ($\alpha=0; \delta=0$, the Heisenberg model HM) of the solid curve can be discarded because it does not describe the susceptibility (cf. Fig. 7). The parameter set ($\alpha=0.12; \delta=0.05$) of the dashed curve seems to fit the data down to $T \approx 0.7J$. For lower values, however, the agreement is poor. So this data set must also be discarded. Note that we refer only to the temperature regime where the extrapolated series yield reliable results.

Thus, we have shown for the above example that it is *not* possible to describe the data of a dynamic spin-phonon system in the intermediate regime, where all energy scales are of similar magnitude, in the framework of static spin models plus (decoupled) phonons. But it is not sufficient to consider only one quantity at (relatively) high temperatures. In order to obtain unambiguous evidence of the presence of a dynamic spin-phonon coupling, one has to dispose of either

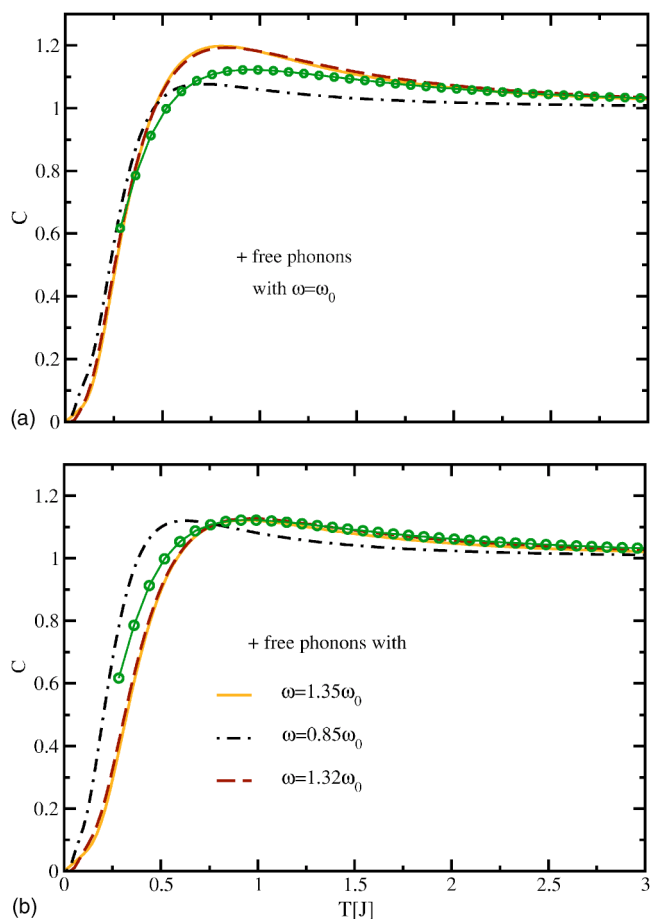


FIG. 8. (Color online) Comparison of the specific heat for the parameter sets determined from the susceptibility in Fig. 8. For the upper plot the phonon frequency is assumed to be known beforehand. For the lower plot no *a priori* knowledge is assumed for the phonon frequency; thus, it is also fitted. The line styles are the same as those used in Fig. 7; that means, the exchange couplings used are those from the corresponding curves in Fig. 7.

data down to low temperatures (not considered here) or to consider at least two independent thermodynamic quantities. Otherwise, one may easily be misled by a good agreement in one quantity alone to conclude that a simpler static model is sufficient for a microscopic description.

IV. SUMMARY AND OUTLOOK

The problem of a one-dimensional spin system coupled to phononic degrees of freedom is investigated. A cluster expansion is applied to obtain a series expansion in the magnetic coupling J . Results are computed at finite temperatures for the free energy, the specific heat, and the magnetic susceptibility. No truncation in the phononic subspace is necessary because the expansion is performed in J about the limit $J=0$, not in the inverse temperature. This is the realization of a cluster expansion at finite temperatures for an extended spin-phonon problem. The implementation of the expansion in a computer program yields high orders in the expansion parameter.

The comparison of the results obtained from the extrapolated series to data from quantum Monte Carlo simulations

shows very good agreement. This supports the reliability of the approach. Hence, our results can serve as input for quantitative data analysis because the features of the magnetic susceptibility and the specific heat at moderate and at high temperatures $T \gtrsim 0.15 - 0.25J$ are described reliably.

A possible route to improve the extrapolations is to understand the limit $J \rightarrow \infty$ in the Hamilton operator (1) better. At first glance, this limit looks simple because it corresponds to the adiabatic situation with $\omega/J \rightarrow 0$. But this limit is not straightforward because the nature of the excitations is unclear at present. Note that in this limit static displacements can be made at no energetic cost. This suggests that the excitations are domain walls. Whether these objects are static (because $\omega/J \rightarrow 0$) or dynamic (because the magnetic subsystem retains its fluctuations) is unclear at present and constitutes an interesting theoretical issue in itself.

Finally, we analyzed the data of a spin-phonon system in the intermediate coupling regime, where all energies are of similar magnitude, in great detail. As expected, we could show that the effects of the dynamic spin-phonon coupling

cannot be imitated by a static spin model and decoupled phonons. But it is necessary to study low temperatures or at least two quantities, such as the susceptibility and the specific heat, carefully. Otherwise, one may be easily misled by a good agreement in one quantity alone to conclude that a static microscopic model is sufficient. We think that this conclusion is helpful for future experimental analyses of low-dimensional spin systems.

ACKNOWLEDGMENTS

We like to thank C. Aits and U. Löw for kindly providing the QMC data as benchmarks. We acknowledge the financial support by the DAAD for an extended visit by one of us (A.B.) to the University of New South Wales where a significant part of this project was carried out. We are indebted to the DFG for the support in SP1073 and SFB608. Last, but not least, G.S.U. gratefully acknowledges the hospitality and the support of the COE at Tohoku University, Sendai, where the manuscript was finished.

*Electronic address: ab@thp.uni-koeln.de

†Electronic address: gu@thp.uni-koeln.de

‡Electronic address: otja@phys.unsw.edu.au

¹E. Pytte, Phys. Rev. B **10**, 4637 (1974).

²J. W. Bray, L. V. Interrante, I. S. Jacobs, and J. C. Bonner, in *Extended Linear Chain Compounds*, edited by J. S. Miller (Plenum Press, New York, 1983), Vol. 3, p. 353.

³M. C. Cross and D. S. Fisher, Phys. Rev. B **19**, 402 (1979).

⁴H. Fröhlich, Proc. R. Soc. London **A223**, 296 (1954).

⁵R. E. Peierls, *Quantum Theory of Solids* (Oxford University Press, Oxford, 1955).

⁶W. P. Su, J. R. Schrieffer, and A. J. Heeger, Phys. Rev. Lett. **42**, 1698 (1979).

⁷M. Hase, I. Terasaki, and K. Uchinokura, Phys. Rev. Lett. **70**, 3651 (1993).

⁸M. Braden, G. Wilkendorf, J. Lorenzana, M. Aïn, G. J. McIntyre, M. Behruzi, G. Heger, G. Dhalenne, and A. Revcolevschi, Phys. Rev. B **54**, 1105 (1996).

⁹W. Geertsma and D. Khomskii, Phys. Rev. B **54**, 3011 (1996).

¹⁰H. Kageyama, K. Yoshimura, R. Stern, N. V. Mushnikov, K. Onizuka, M. Kato, K. Kosuge, C. P. Slichter, T. Goto, and Y. Ueda, Phys. Rev. Lett. **82**, 3168 (1999).

¹¹S. Miyahara and K. Ueda, J. Phys. Soc. Jpn. **69**, 72(Suppl.B) (2000).

¹²A. W. Garrett, S. E. Nagler, D. A. Tennant, B. C. Sales, and T. Barnes, Phys. Rev. Lett. **79**, 745 (1997).

¹³M. Grove, P. Lemmens, G. Güntherodt, B. C. Sales, F. Bülesfeld, and W. Assmus, Phys. Rev. B **61**, 6126 (2000).

¹⁴G. S. Uhrig and B. Normand, Phys. Rev. B **63**, 134418 (2001).

¹⁵R. J. Bursill, R. H. McKenzie, and C. J. Hamer, Phys. Rev. Lett. **83**, 408 (1999).

¹⁶G. S. Uhrig, Phys. Rev. B **57**, R14004 (1998).

¹⁷C. Raas, A. Bühler, and G. S. Uhrig, Eur. Phys. J. B **21**, 369 (2001).

¹⁸C. Raas, U. Löw, G. S. Uhrig, and R. W. Kühne, Phys. Rev. B **65**,

144438 (2002).

¹⁹A. Weiße, G. Wellein, and H. Fehske, Phys. Rev. B **60**, 6566 (1999).

²⁰S. Trebst, N. Elstner, and H. Monien, Europhys. Lett. **56**, 268 (2001).

²¹P. Sun, D. Schmeltzer, and A. R. Bishop, Phys. Rev. B **62**, 11308 (2000).

²²A. W. Sandvik, R. R. P. Singh, and D. K. Campbell, Phys. Rev. B **56**, 14510 (1997).

²³R. W. Kühne and U. Löw, Phys. Rev. B **60**, 12125 (1999).

²⁴A. W. Sandvik and D. K. Campbell, Phys. Rev. Lett. **83**, 195 (1999).

²⁵C. H. Aits, *Quanten-Monte-Carlo Untersuchungen effektiver Spinmodelle mit Spin-Phonon Kopplung* (Diplomarbeit, Köln, 2002).

²⁶C. H. Aits and U. Löw, Phys. Rev. B **68**, 184416 (2003).

²⁷A. Bühler, *Hochtemperaturentwicklung für Spinketten und effektive Spinmodelle für Spin-Peierls-Systeme* (Diplomarbeit, Köln, 1999), available at <http://www.thp.uni-koeln.de/~gu/diploma.html>

²⁸R. Werner, C. Gros, and M. Braden, Phys. Rev. B **59**, 14356 (1999).

²⁹C. Domb and M. S. Green, eds., *Phase Transitions and Critical Phenomena* (Academic Press, New York, 1974), Vol. 3.

³⁰A. Klümper, Z. Phys. B: Condens. Matter **91**, 507 (1993).

³¹S. Eggert, I. Affleck, and M. Takahashi, Phys. Rev. Lett. **73**, 332 (1994).

³²A. Klümper, Eur. Phys. J. B **5**, 677 (1998).

³³A. Bühler, U. Löw, and G. S. Uhrig, Phys. Rev. B **64**, 024428 (2001).

³⁴G. Castilla, S. Chakravarty, and V. J. Emery, Phys. Rev. Lett. **75**, 1823 (1995).

³⁵J. Riera and A. Dobry, Phys. Rev. B **51**, 16098 (1995).

³⁶K. Fabricius, A. Klümper, U. Löw, B. Büchner, T. Lorenz, G. Dhalenne, and A. Revcolevschi, Phys. Rev. B **57**, 1102 (1998).